THREE-DIMENSIONAL STRUCTURES OF SUBSTITUTED BENZYLPHENYL ETHERS

Bohdan SCHNEIDER[a], Karel HUML[b] and Václav REJHOLEC[a]

[a] *Research Institute for Pharmacy and Biochemistry, 130 60 Prague 3*
[b] *Institute of Macromolecular Chemistry, Czechoslovak Academy of Sciences, 162 06 Prague 6*

Received July 20, 1990
Accepted April 4, 1991

Forty nine three-dimensional crystal structures of a benzylphenyl ether fragment retrieved from the Cambridge Structural Database were confronted with computed conformational maps of the fragment. Due to the symmetry the number of analyzed fragments rose to 98. When an endocyclic torsion angle of a phenyl ring deviates from 0° the adjacent torsion angle is deformed in opposite direction compensating thus the deviation from planarity. The shape of the fragment is mainly controlled by torsion angles τ_1 = C–C–O–CH_2, τ_2 = C–O–CH_2–C, and τ_3 = = O–CH_2–C–C. The attachment of both phenyl rings to the –CH_2–O– moiety is not symmetrical and the deformation depends on the value of the τ_3 angle. In the crystal, the fragment prefers conformations with τ_1 around 0°, τ_2 around 180° and with broad bimodal distribution of τ_3 around 0° and ±90° despite the fact that energetically equivalent regions exist in the potential energy maps for τ_2 values near 60° and 300° and that many crystal structures with τ_3 around 0° lie in higher energetical regions than those with τ_3 around 90°. Thus a significant difference between the crystal and simulated gas phase conformations was observed supporting the hypothesis that crystals prefer flatter and more storable molecular conformations.

The importance of three-dimensional molecular structures for explanation of biological properties of compounds is widely accepted. A way how to causally connect structures and properties of molecules is, however, disputable. We feel that the very first step in understanding these structure–activity relationships should be a detailed description of structural features of relevant molecules.

In the recent paper[1], we described the geometry of diphenyl sulfide molecules. The present paper is an attempt to treat a more complicated system of benzylphenyl ether preserving the approach of that communication[1].

Various compounds of a type phenyl–$(CH_2)_n$–O–phenyl were studied in connection with their antiinflammatory activity using QSAR methodology[2], especially those carboxy-substituted at the phenyl rings. Differences in calculated and observed parameters of lipophilicity or its logarithm led to a hypothesis that intramolecular interactions were involved, causing partial failure of the additivity principle. These effects were observed in aromatic compounds with two or more aromatic nuclei[3]. Provided that the molecular structures allow mutual approach of the phenyl rings

the differences in lipophilicity can be explained by intramolecular hydrophobic interaction decreasing the hydrophobic molecular surface which in turn increases solubility in the water phase. The original purpose of the paper was to look for intramolecular interactions of the benzene rings of the benzylphenyl ether molecules. During progress of the work[4] we comprehended, however, that much more detailed analysis of geometrical parameters of the fragment would be necessary.

Seeking for general rules of geometrical behaviour of substituted benzylphenyl ethers, precise molecular geometries are needed. Therefore we analyzed molecular geometries determined by X-ray crystallography and simulated by molecular mechanics calculations. Describing geometry of any molecule, proper geometrical parameters had to be chosen and their contingent relations found. A relation between experimental and calculated conformations was examined as well.

METHODS

Database search. A fragment of general formula *I* (Fig. 1) was searched in the January 1989 version of the Cambridge Structural Database[6] using the QUEST89 program[6]. A list of 38 compounds containing the fragment is in Table I. In these 38 compounds, the GSTAT89 program[6] identified 49 benzylphenyl ether fragments *I*. This program was also used to calculate all interesting geometric parameters of the fragment*.

Symmetry of the fragment I. The numbering of both phenyl rings of the fragment is not unambiguous (see numbering scheme in Fig. 1) or — in other words — the fragment has some possible symmetry. Thus some of the raw geometric data obtained from GSTAT89 had to be transformed. Handling of bond angles and distances is simple since transformed values are

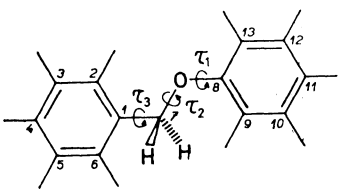

I

FIG. 1

Definition of geometrical parameters used for description of the benzylphenyl ether fragment *I* and its labeling scheme:
τ_1 = C7–O–C8–C9; τ_2 = C1–C7–O–C8; τ_3 = C2–C1–C7–O; ω_{C1} = C6–C1–C2–C3; ω_{C2} = = C1–C2–C3–C4; ω_{C3} = C2–C3–C4–C5; ω_{O1} = C13–C8–C9–C10; ω_{O2} = C8–C9–C10–C11; ω_{O3} = C9–C10–C11–C12; ω_C = C7–C1–C2–C3; ω_O = O–C8–C9–C10; Δ_C = (C2–C1–C7)— —(C6–C1–C7); Δ_O = (C9–C8–O) — (C13–C8–O); φ oriented angle of the phenyl rings

* The search question as well as bibliography and values of all geometrical parameters of compounds containing the benzylphenyl ether fragment are available upon request from one of the authors (B.S.).

TABLE I

A list of reference codes and chemical names of compounds containing the benzylphenyl ether fragment *I*

No.	Code	Chemical name
1—2	BAGDIW	(1*S*)-spiro(4-O-(β-D-galactopyranosyl)-1-dehydroxy-D--glucopyranose-1,1′-(5,7-bis(*p*-bromobenzyloxy)-2′-oxaindane
3	BEDKIE	ethyl *trans*-7-benzyloxy-4-hydroxy-6-methoxy-1-(3,4,5-trimethoxyphenethyl)-1,2,3,4-tetrahydro-2-isoquinolinecarboxylate
4—5	BOFSEU	3-(4-((3-nitrophenyl)-methoxyphenyl))-6-methoxymethyl--2-oxazinone
6	BOGJIO	4,10-dioxo-4β-chloro-5-(benzyloxy)-9β-hydroxy-9α-methyl--1,4,9,9α,10-pentahydroanthracene
7	BOJKIU	3-(4-((3-chlorophenyl)methoxy)phenyl)--8-(methoxymethyl)-2-oxazolidinone
8	BOJKOA	3-(4-((3-cyanophenyl)methoxy)phenyl)--5-(methoxymethyl)-2-oxazolidinone
9	BOKLAO	1-benzyloxy-3-methyl-4-nitrobenzene
10	BOLFOX	2-(4-(4-chlorophenoxymethyl)phenoxy)propionic acid
11	BUGJIW	5-(methoxymethyl)-5-methyl-3-(4-((3-nitrophenyl)-methoxy)phenyl-2-oxazolidinone
12	BUHGEQ	5-(1-methyl)methoxymethyl-3-(4-((3-cyanophenyl)-methoxy)phenyl)-2-oxazolidinone
13—14	CADGET	1,4,7,14,22-pentaoxa[7]orthocyclo-[2]metacyclo[2]orthocyclophane
15—16	CEYKIA	(*E*)-1,2 : 5,6 : 9,10-tribenzo-3,4-dimethyl--7,12-dioxacyclododeca-1,3,5,9-tetraene
17—18	CEYKOG	(*Z*)-1,2 : 5,6 : 9,10-tribenzo-3,4-dimethyl--7,12-dioxacyclododeca-1,3,5,9-tetraene
19—20	CIDXIW	(4-(benzyloxy)phenyl)acetic acid
21	CIDXOC	(4-(phenoxymethyl)phenyl)acetic acid
22	COXBIA	1-oxa-10-thia(2,2)metacyclophane
23	COYTOZ	(4*R*)-3-(4-((3-chlorophenyl)methoxy)phenyl)-5--(methylaminomethyl)-1,3-oxazolidin-2-one methanesulfonic acid
24	COYTUF	*trans*-3-(4-(5-methoxymethyl-4-methyl-2-oxo-1,3-oxazolidin--3-yl)phenoxymethyl)benzonitrile

TABLE I
(*Continued*)

No.	Code	Chemical name
25	COYVAN	*cis*-3-(4-(5-methoxymethyl-4-methyl-2-oxo-1,3-oxazolidin--3-yl)phenoxymethyl)benzonitrile (different crystal modification of COYTUF)
26—28	CUDXUU	17,17,40,40-tetramethyl-7,30-dinitro-1,10,24,33-tetraoxa-(2.2.1.2.2.1)*meta-para-para-meta-para-para*-cyclophane benzene clathrate
29—30	CUFYUX	*cis*-6,11,17,18-tetrahydro-5-12-dioxatribenzo-(a,e,i)cyclododecene-17,18-diol
31	CUHYUZ	(5*R*,1*R*)-5-(1-methylmethoxymethyl)-3-(4-(3-cyanophenyl--methoxy)phenyl)oxazolidin-2-one
32	CUNMAZ	4-benzyloxy-3-hydroxybenzaldehyde
33—34	CUNSOT	2,2′-(O-phenylene-bis(methyleneoxy))diacetophenone
35	CUYFAD	3,17β-dibenzyloxy-9β-methoxy-11-estra--1,3,5(10)-trien-11-one
36	CXBTZE20	4,6-diamino-1-(3-chloro-4-(*m*-dimethylcarbamoyl-benzyloxy)phenyl)-1,2-dihydro-2,2-dimethyl-*s*-triazine ethanesulfonate
37—38	DAXMOE	6,13,20,23,26,29,32,34,37,40,43,46-dodecaoxapentacyclo--octatetraconta-1(2),3,7(8),9,11,15(16),17,19(48),33(47)-nonaene
39	DEBTUZ	(*Z*)-4,5-dihydro-2-(2-phenyl-2-(4-benzyloxyphenyl)-cyclopropyl-1*H*-imidazole diethyl ether solvate
40—41	DEHHON	(3*R*)-1-((1*R*)-(*p*-benzyloxyphenyl)-benzyloxycarbonylmethyl)-3-isopropenylazetidin-2-one
42	DETGIS	3-(*p*-benzoyloxyphenyl)sydnone
43	DEZNOL	(*E*)-3-((4-(5-methoxymethyl-2-oxo-tetra-hydrofuran-3-yl)phenoxy)methyl)benzonitrile
44	DEZNUR	(*Z*)-3-((4-(5-methoxymethyl-2-oxo-tetra-hydrofuran-3-yl)phenoxy)methyl)benzonitrile
45	DMEWAR10	dimethylwariftein
46	DORLUR	7-benzyoloxy-6,2′,3′,4′-tetramethoxyisoflav-3-ene
47	FIKCIL	4′-hydroxymethyl-5-benzyloxybenzylacyclouridine
48	MBAUTM	3-methyl-mono-O-benzylautumnaline
49	MWARIF10	methylwariftein

arithmetic means of symmetry-equivalent parameters. For example, the valence bonds C2–C3 and C5–C6 as well as the valence angles C2–C3–C4 and C4–C5–C6 are considered being equivalent. A proper treatment of other parameters is, however, more complicated.

For symmetry considerations, the key parameters were torsion angles τ_1, τ_2, and τ_3 (for definitions of parameters, see Fig. 1). At the beginning, τ_1 and τ_3 were corrected for nonplanarity of the phenyl rings:

$$\tau_i \rightarrow \tau_i + \{|\tau_i - \tau_i'| - 180°\}/2\,, \qquad (1)$$

where $i = 1, 3$ and τ_i' is an "adjacent" torsion to τ_i: e.g. for τ_1 = C7–O–C8–C9 is τ_1' = C7–O–C8–C13. Symmetric behaviour of τ_1, τ_2, and τ_3 was described by the Dunitz method[7] considering both phenyl rings as rigid regular hexagons. The symmetry of a conformational space of the fragment is then isomorphous to the three-dimensional crystallographic space group $P1$ with unit cell axes corresponding to τ_1, τ_2, and τ_3 torsion angles, respectively. Rotational periodicity of torsion angles is converted to translational symmetry of a space group. Lengths of the unit cell axes are 180° for τ_1 and τ_3 and 360° for τ_2. The particular unit cell used for conformational analysis was that from −90° to +90° for τ_1 and τ_3 and from 0° to 360° for τ_2.

All τ_1 and τ_3 values lying out of the interval $\langle -90°, +90° \rangle$ were transferred to this interval by renumbering the fragment *I* or by algebraic operation. Both ways are equivalent. When for instance τ_1 is to be transformed one of the following operations has to be done.

Renumbering	Calculation
C9 → C13	$\tau_1 < -90°$: $\tau_1 \rightarrow \tau_1 + 180°$
C10 → C12	$\tau_1 > +90°$: $\tau_1 \rightarrow \tau_1 - 180°$

Transformations of τ_3 are fully analogical. Transformations of τ_1 or τ_3 angles to the interval $\langle -90°, +90° \rangle$ necessitate transformations of other parameters, too. The transformations can be most easily explained in terms of fragment renumbering. In the case that τ_1 was transformed, the following set of equations holds (Eq. (2)):

$$\tau_1 = \text{C7–O–C8–C13}; \quad \omega_O = \text{C12–C13–C8–O}; \qquad (2)$$

$$\Delta_O = \text{(C13–C8–O)–(C9–C8–O)}$$

$$\omega_{O1} = \text{C9–C8–C13–C12}; \quad \omega_{O2} = \text{C8–C13–C12–C11}; \quad \omega_{O3} = \text{C13–C12–C11–C10}.$$

Transformations compelled by transferring τ_3 to the interval $\langle -90°, +90° \rangle$ affect parameters ω_C, Δ_C, ω_{C1}, ω_{C2}, and ω_{C3} by a way similar to the transformations shown in Eqs (2).

In the next step, the symmetry equivalent positions of the space group $P1$ were created for all conformations:

$$[\tau_1, \tau_2, \tau_3] \rightarrow [-\tau_1, 360 - \tau_2, -\tau_3]\,. \qquad (3)$$

The total number of analyzed fragments is thus two times the number of identified fragments. As a consequence of generation of equivalent positions in the conformational space (τ_1, τ_2, τ_3) (see Eq. (3)), an original set of other parameters had to be symmetrized, too.

$$\omega_O \rightarrow 360 - \omega_O; \quad \omega_C \rightarrow 360 - \omega_C; \quad \Delta_O \rightarrow \Delta_O; \quad \Delta_C \rightarrow \Delta_C \qquad (4)$$

$$\omega_{O1} \rightarrow -\omega_{O1}; \quad \omega_{O2} \rightarrow -\omega_{O2}; \quad \omega_{O3} \rightarrow -\omega_{O3}$$

$$\omega_{C1} \rightarrow -\omega_{C2} \quad \omega_{C2} \rightarrow -\omega_{C2} \quad \omega_{C3} \rightarrow -\omega_{C3}$$

After transformations (Eq. (2)) and symmetrization (Eqs (3) and (4)), all the studied data was arranged to a data matrix. Rows of the data matrix consist of parameter values for a particular fragment and its columns are composed of values of a particular parameter in all fragments. Each fragment appears twice in the data matrix and the number of the analyzed fragments is therefore 98.

Molecular mechanics calculations. An empirical force field method of molecular mechanics[8] was used to simulate conformational behaviour of the benzylphenyl ether molecule because of its reliability and computational efficiency. We used the MMPMI program[9] modified for IBM PC computers[10]. Three two-dimensional sections $E = E(\tau_i, \tau_j)$ of the conformational map $E = E(\tau_1, \tau_2, \tau_3)$ were computed at points $[\tau_i, \tau_t]$ with τ_i, and τ_j values systematically changed by the dihedral driver option of the program in steps of 15°. All other geometrical parameters were fully refined at all $[\tau_i, \tau_j]$ points of the maps.

RESULTS AND DISCUSSION

Distributions of the "bridge" bond lengths d_1, d_2, and d_3 are unimodal with average values of 1·337 (14), 1·428 (20), and 1·504 (19) Å, respectively (estimated standard deviations in parentheses) which are in agreement with the expected values[11]. A large span of distributions of d_1 (1·355 – 1·429 Å), d_2 (1·379 – 1·480 Å), and d_3 (1·439 – 1·576 Å) indicates that values can deviate significantly from their mean values. The same applies for bond angles α_O and α_C: Extrema are 110·4° and 121·4° for α_O and 102·9° and 114·5° for α_C and their arithmetic means [117·5 (2·2)° and 108·6 (2·1)°, respectively] do not depart from expected values.

Planarity of the Phenyl Rings

Torsion angles ω describe deformations of the phenyl rings from planarity (for definitions, see Fig. 1). A significant correlation between adjacent torsion angles ω was observed for both phenyl rings. Inside a ring, the correlation coefficients vary from −0·62 (F = 29·1, 48 degrees of freedom, DF) for the ω_{O3} on ω_{O2} dependence to −0·80 (F = 80·9, 48 DF) for the ω_{O2} on ω_{O1} dependence. These correlations are interpreted as a tendency of the phenyl rings to counterbalance distortions from planarity deforming adjacent torsion angles in opposite directions.

In the case of the planar sp^2 arrangement on the C1 and C8 phenyl atoms, a linear dependence between ω_O and ω_{O1} and between ω_C and ω_{C1} should be observed. Actual values of correlation coefficients (0·66 and 0·72) confirm effectively planar arrangement of C1 and C8 but significant deviations occured (especially in structures coded BAGDIW, MBAUTM, and COXBIA, see Table I).

Unsymmetrical Attachment of the Phenyl Rings to the $-CH_2-O-$ *Moiety*

Deformation angles Δ_O and Δ_C have unsymmetrical distributions with the arithmetic means of 4·1 (1·6)° and 1·1 (1·3)°. Asymmetry of the $-CH_2-$ group attachment to

the phenyl is smaller than that of the ether –O– group and is marginal. Prevailing positive values of both parameters are the corollary of overcrowding of C9 substituents and hydrogens of the "bridge" $-CH_2-$ group and of C2 substituents and oxygen lone electron pairs (see Fig. 1). A slight dependence between Δ_O and Δ_C was observed: For large positive values of Δ_O, the values of Δ_C are lowest while for positive values of Δ_C, Δ_O has the smallest values. The scattergram of Δ_O vs Δ_C and correlation lines are depicted in Fig. 2. Leaving out of account the point [−1·5°, −0·5°], the linear correlation coefficient r for the dependency of Δ_O on Δ_C is −0·50 (F = 15·2, 47 DF).

As will be shown later, the values of the torsion angle τ_3 form two clusters. Respecting the existence of these two clusters, fragments were divided into two groups. The dependence of Δ_O on Δ_C is different in each cluster. For fragments with the τ_3 values around 90°, the distribution of both deformation angles Δ_O and Δ_C are wider and the correlation is significantly tighter (r = −0·76, F = 34·7, 26 DF) than for fragments with τ_3 near 0° (r = −0·49, F = 10·3, 20 DF). Similar behaviour of deformation angles Δ was described in the diphenyl sulfide fragment[1] when the largest values of the angle Δ were observed for conformations with one of the C–S–C–C torsion angles near 0° when the repulsion of the phenyl rings is largest.

Experimental Distributions and Computed Conformational Space of the Torsion Angles τ_1, τ_2, and τ_3

The overall shape of the fragment is mainly controlled by three torsion angles τ_1, τ_2, and τ_3. Histograms of their values along with values of the dihedral angle φ between phenyl ring planes are in Fig. 3. A broad distribution of the angle φ suggests that mutual orientation of the phenyls does not play a significant role in stabilizing

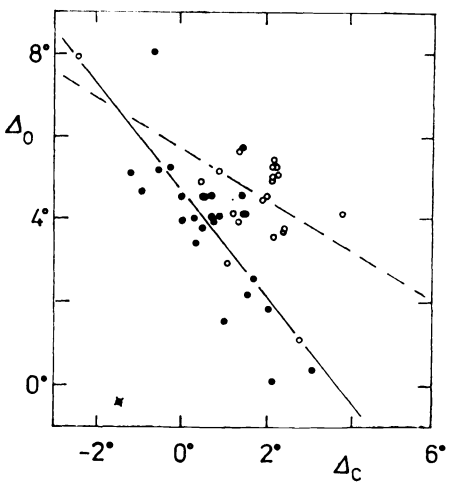

FIG. 2

Scattergram of deformation angles Δ_O vs Δ_C. Empty points belong to the fragments with the τ_3 values near 0° and corresponding linear regression is indicated by the dashed line. Points for fragments with τ_3 near 90° are designated by full points and the regression line is full

the fragment. Orientations of the torsion angles τ_1, τ_2, and τ_3 are on the contrary limited and correlated. The angle τ_2 has the narrowest distribution with some distant outliers around 60° and 300°. The distribution of τ_1 is wider but number of outliers is the same as in the case of τ_2 – 12. Both torsions show preference of the phenyl–$-O-CH_2-$ moiety for a planar arrangement. The distribution of the angle τ_3 is however very wide and indicated existence of at least two clusters: around 0° and $\pm 90°$.

The scattergrams of the torsion angles τ_1, τ_2, and τ_3 are in Figs 4–6. The scattergram of τ_1 vs τ_2 breaks to two parts: A compact region near the point [0°, 180°] with significantly correlated points ($r = -0{\cdot}77$, $F = 116, 81$ DF) and sixteen widely distributed outliers (two fragments of structure CUDXUU superimpose in the scattergram but otherwise are not identical). The central clump is projected on to a valley of low enthalpies. Although the correlation of τ_2 with τ_1 is statistically significant it does not seem to have any simple explanation in terms of the shape of the potential energy map. Energetically almost equivalent valleys at the τ_2 values of 60° and 300° are occupied by only six structures each and none of the structures lie closely to the local minimum. The only apparent difference between the minimum at [0°, 180°] and those at [30°, 60°] and [−30°, 300°] is in the shapes of the phenyl–$-O-CH_2-$ moiety. Nonplanar and highly "folded" conformations with τ_2 around

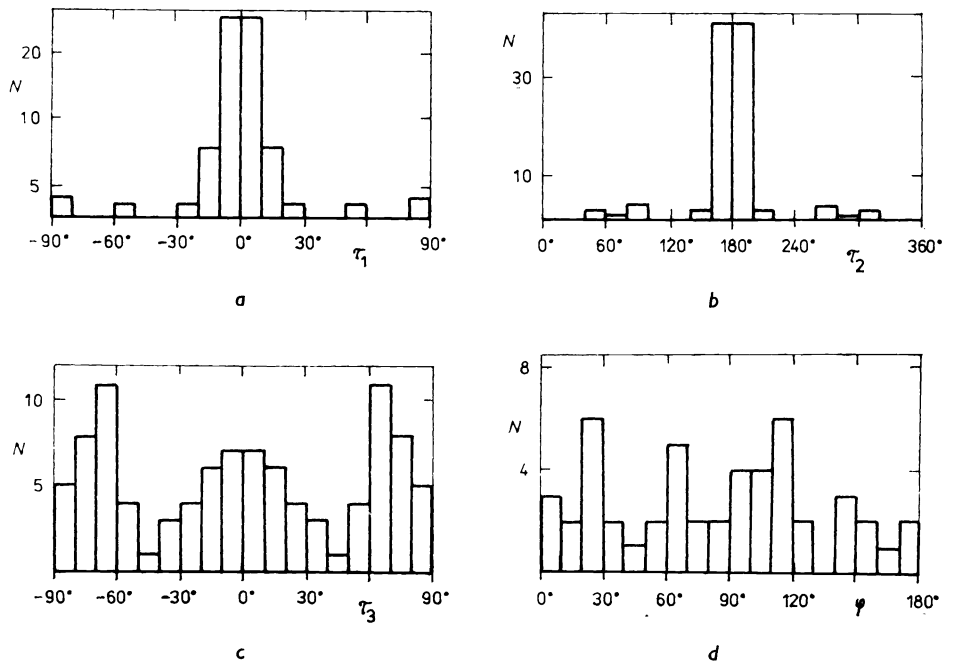

FIG. 3

Histograms of torsion angles $\tau_1(a)$, $\tau_2(b)$, $\tau_3(c)$, and of dihedral angle $\varphi(d)$

60° or 300° are probably less storable than the "open" conformation with τ_2 around 180° which might be the explanation of observed strong preference for "open" conformations in the crystals. This view is supported by the fact that only two out of twelve τ_2 outliers come from molecules not having macrocyclic structure (FIKCIL,

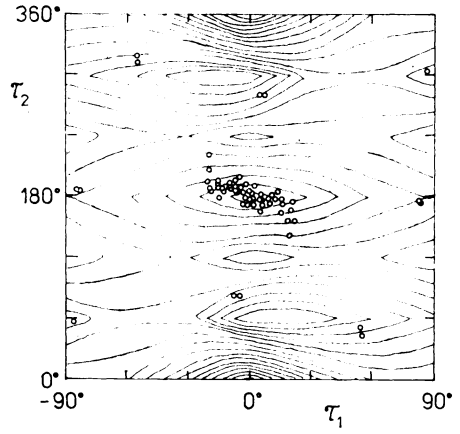

FIG. 4

Superposition of experimental points $[\tau_1, \tau_2]$ and curves of constant enthalpy of formation for the two-dimensional conformational map $E = E(\tau_1, \tau_2)$ of the benzylphenyl ether. Curves are plotted in 2 kJ/mol steps from the minimal value of 55·7 kJ/mol

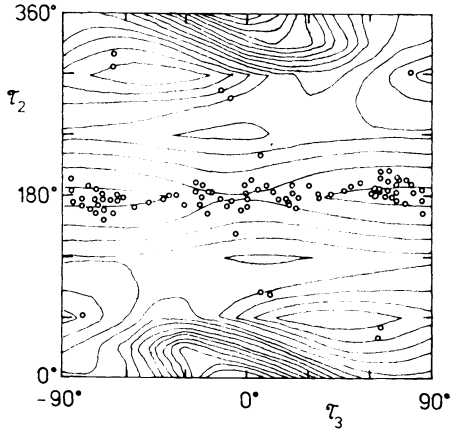

FIG. 5

Superposition of experimental points $[\tau_3, \tau_2]$ and curves of constant enthalpy of formation for the two-dimensional conformational map $E = E(\tau_3, \tau_2)$ of the benzylphenyl ether. Curves are plotted in 3 kJ/mol steps from the minimal value of 54·8 kJ/mol

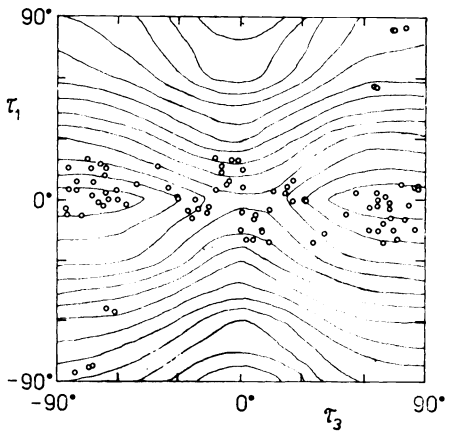

FIG. 6

Superposition of experimental points $[\tau_3, \tau_1]$ and curves of constant enthalpy of formation for the two-dimensional conformational map $E = E(\tau_3, \tau_1)$ of the benzylphenyl ether. Curves are plotted in 1 kJ/mol steps from the minimal value of 56·5 kJ/mol

all other are macrocycles: COXBIA, CUDXUU 2X, DMEWAR10, MWARIF10, each fragment appears twice in the maps). The macrocyclic structures are stabilized in "folded" conformations by covalent bonds to other parts of the molecules.

The topography of the conformational map $E = E(\tau_3, \tau_2)$ is very similar to that of the map $E = E(\tau_1, \tau_2)$ with the exception of switched positions of the minimum and the saddle point in the valley along $\tau_2 = 180°$ (Fig. 5). The energetic difference between the minimum and the saddle point is lower for the $E(\tau_3, \tau_2)$ than for $E(\tau_1, \tau_2)$ map (6 and 10 kJ/mol, respectively). Small energetic differences along the $\tau_2 = 180°$ valley can apparently be compensated by intermolecular forces in the crystal which explains the existence of two clusters of the τ_3 values: The first cluster naturally lies in the energetically most favorable region around $\tau_3 \pm 90°$. The position of the second one seems to support our hypothesis about the preference of planar conformations in crystals since conformations with τ_3 around 0° are more planar and thus more storable. The sporadic occurence of the experimental points in the local minima at τ_2 60° and 300° has already been discussed in connection with the map $E = E(\tau_1, \tau_2)$.

The τ_3 vs τ_1 scattergram shows again two broad clusters of points around $\pm 90°$ and 0° (Fig. 6). The corresponding conformational map is however much simpler and flatter than those comprising τ_2 (compare Figs 4, 5, and 6) containing only one minimum at [0°, ±90°] and two saddle points at [0°, 0°] and [±90°, ±90°]. Barriers along the $\tau_1 = 0°$ valley are very low and the saddle point is only about 4 kJ/mol above the minimum. A shift along τ_3 does not significantly destabilize conformations with $\tau_1 = 0°$. Even the conformations climbing toward the other saddle point, which is 9·5 kJ/mol above the minimum, are energetically accessible. Their rare occurence is again more a matter of interactions in the crystals than of energy of the isolated fragment. All outliers in the τ_1 values belong to macrocyclic molecules (CEYKIA 2X, COXBIA, DMEWAR10, and MWARIF10). A substantial overlap is revealed between the structures forming τ_1 and τ_2 outliers: three of eight fragments have unusual values for both these angles (COXBIA, DMEWAR10, and MWARIF10).

CONCLUSIONS

(i) The torsion angles of both phenyl rings of the benzylphenyl ether fragment can deviate significantly from planarity. The adjacent torsion angle, however, tend to be deformed in the opposite direction compensating thus the deviations from planarity. (ii) The attachment of the phenyl rings to the $-CH_2-O-$ moiety is not symmetrical and the deformation depends on the value of τ_3 torsion angle. (iii) The substantial difference was observed between the (simulated) gas phase and solid phase conformational spaces of the fragment. In the crystal, the fragment prefers flatter shape with torsion angles τ_1 around 0° and τ_2 around 180° and with broad distribution of τ_3 making two clusters around 0° and ±90°. Energetically equivalent

regions are predicted by molecular mechanics for the τ_2 values at 180° as well as near 60° and 300°. Only the valley at 180° is occupied by the crystal conformations, though. Further, experimental conformations with τ_3 around 0° lie in energetically less favourable regions than the available around $\tau_3 = 90°$. We believe that this supports the view that crystals prefer more storable conformations of molecules over conformations which are equally or even little more energetically stable for isolated molecules in the gas phase but which are bulkier.

REFERENCES

1. Schneider B., Rejholec V., Kuchař M.: Collect. Czech. Chem. Commun. *55*, 2590 (1990).
2. Kuchař M., Rejholec V., Roubal Z., Němeček O.: Collect. Czech. Chem. Commun. *44*, 183 (1973).
3. Canas-Rodrigues A., Tute M. S.: Adv. Chem. Ser. *114*, 41 (1972).
4. Schneider B., Hašek J., Huml K.: Z. Kristallogr. *185*, 151 (1988).
5. Allen F. H., Bellard S., Brice M. D., Cartwright B. A., Doubleday A., Higgs H., Hummelink T., Hummelink-Peters B. G., Kenard O., Motherwell W. D. S., Rodgers J. S., Watson D. G.: Acta Crystallogr., B *35*, 2331 (1979).
6. *Cambridge Structural Database System.* Cambridge Crystallographic Data Center, Cambridge 1989.
7. Dunitz J. D.: *X-Ray Analysis and the Structure of Organic Molecules.* Cornell University Press, Ithaca 1979.
8. Burkert U., Allinger N. L.: *Molecular Mechanics. ACS Monograph 177.* American Chemical Society, Washington D.C. 1982.
9. QCPE Program, Nos. 395 and 318. QCPE, Bloomington 1977.
10. Gilbert K. E., Gajewski J. J.: *A MMPMI Molecular Mechanics Program.* Indiana University, Indiana 1985.
11. Allen F. H., Kennard O., Watson D. G., Brammer L., Orpen A. G., Taylor R.: J. Chem. Soc., Perkin Trans. 2 *1987*, S1.

Translated by the author (B.S.).